PFC/JA-88-41

Periodic Interactions of Charged Particles With Localized Fields—–The Spatial Standard Map

Ram, A. K.; Bers, A.; Kupfer, K.

November 1988

Plasma Fusion Center
Massachusetts Institute of Technology
Cambridge, Massachusetts 02139 USA

This work was supported in part by the National Science Foundation, Grant ECS-8515032 and in part by the Department of Energy Contract No. DE-AC02-78ET-51013.Reproduction, translation, publication, use and disposal, in whole or part, by or for the United States government is permitted.

Submitted for publication in: Physics Letters A.

Table of Contents

PERIODIC INTERACTIONS OF CHARGED PARTICLES WITH LOCALIZED FIELDS—THE SPATIAL STANDARD MAP

A. K. Ram, A. Bers, and K. Kupfer

Plasma Fusion Center and Research Laboratory of Electronics

Massachusetts Institute of Technology

Cambridge, MA 02139 USA

ABSTRACT

We derive and analyze a generic mapping for the spatially periodic interaction of charged particles with localized, coherent electric fields. For such interactions stochastic motion exists in a bounded region of phase-space. Conditions are determined for which diffusion can describe the dynamics in such a bounded, stochastic phase-space.

INTRODUCTION

The spatially periodic interaction of charged particles with a coherent electric field wavepacket of finite spatial extent is of considerable practical interest for plasma heating and current drive. Several models representing this wave-particle interaction have been analyzed [1, 2]. However, because of the finite spatial extent of the fields, many details of the particle dynamics could not be treated analytically. In particular, the definition and evaluation of phase-space diffusion have varied and remained unresolved. In this paper we develop a model consisting of a charged particle interacting periodically with a spatially impulsive (i.e. a delta-function in space), sinusoidally time-varying field. The periodicity length is the spatial separation between two such localized fields and is a constant. This system lends itself to an extensive analytical and numerical treatment primarily because the mapping equations (representing the change in the dynamical variables after each interaction of the particle with the impulsive force) can be explicitly derived. In the following sections we derive the mapping equations and the conditions that would lead to stochastic motion of the particles. The stability conditions for the existence of the primary islands are also derived, and we determine the diffusion coefficient for particles in the stochastic region of phase-space. We find that the concept of diffusion can only exist for amplitudes of the field that are smaller than a critical amplitude. For amplitudes larger than the critical amplitude, the description of the dynamics in terms of an effective diffusion coefficient breaks down. This is primarily due to the fact that the entire phase-space of particle motion cannot become stochastic for a finite amplitude of the field (this is similar to the behavior observed in the Fermi map [3]). The existence of these phase-space boundaries which limit the region of stochasticity result in a breakdown of the diffusion model for large amplitudes.

The map we describe is very different from the standard Chirikov-Taylor map [4] which corresponds to the *temporally* periodic and impulsive interaction of a charged particle with a field that varies sinusoidally in space. Furthermore, in the Chirikov-Taylor map the entire phase-space becomes stochastic above a certain amplitude and diffusion coefficients can be explicitly evaluated for all amplitudes above the critical amplitude for global stochasticity [5].

THE DYNAMICAL MODEL AND THE MAPPING EQUATIONS

The model that we consider describes the one-dimensional motion of a charged particle that is acted upon by a spatially-localized, impulsive, time dependent electric field that is periodic in space. The equation of motion is:

$$\frac{dv}{dt} = \frac{eEL}{m} cos\ (\omega t) \sum_{n=-\infty}^{\infty} \delta(z - nL) \tag{1}$$

where $dz/dt = v$, e and m are the charge and mass, respectively, of the particle, E is the strength of the electric field with frequency ω, and L is the spatial periodicity length that separates the impulsive kicks. By normalizing z to the length L, the time t to $2\pi/\omega$, and the velocity v to $\omega L/2\pi$, (1) can be written in the dimensionless form:

$$\frac{dv}{dt} = \epsilon\ cos(2\pi t) \sum_{n=-\infty}^{\infty} \delta(z - n) \tag{2}$$

where $\epsilon = (eE/mL)(2\pi/\omega)^2$, and v, z, t are now dimensionless variables. The spatial periodicity can be used to express the right-hand side of (2) as a Fourier series, so that the equation of motion becomes:

$$\frac{dv}{dt} = \epsilon \sum_{n=-\infty}^{\infty} cos 2\pi(nz - t) \tag{3}$$

Thus, (2) is equivalent to describing the motion of a charged particle (charge, $+\ e$) that is acted upon by an infinite number of plane electrostatic waves of equal amplitudes but whose (normalized) phase-velocities are: $(V_{ph})_n = 1/n \ \ (n = 0, \pm 1, \pm 2, ...)$.

In order to integrate (2) and derive the corresponding mapping equations, it is easier to rewrite the equations of motion such that the kinetic energy, v^2, and the time, t, are dependent variables and the spatial coordinate, z, is the independent variable. Letting $v^2 = u$, the equations of motion are then:

$$\frac{du}{dz} = 2\epsilon\ cos(2\pi t) \sum_{n=-\infty}^{\infty} \delta(z - n) \tag{4}$$

$$\frac{dt}{dz} = \frac{1}{\sqrt{u}} \tag{5}$$

The above equations can be solved easily to give the mapping equations:

$$u_{n+1} = u_n + 2\sigma\epsilon\ cos2\pi t_n \tag{6}$$

$$t_{n+1} = t_n + \frac{1}{\sqrt{u_{n+1}}} \qquad \text{mod } 1 \tag{7}$$

where u_{n+1} is the energy of the particle after it has received its n-th impulse and t_{n+1} is the time (or the phase of the wave) at which it arrives at the position where it receives its $(n+1)$-th impulse. σ is either 1, or 0, or -1 and is related to the direction of the velocity of the particle. For particles with positive velocity $\sigma = 1$ and for particles with negative velocity $\sigma = -1$. When a particle suffers a reflection, i.e. there is a reversal in the direction of the velocity of the particle at the position of an impulse, $\sigma = 0$. We shall refer to the mapping equations (6) and (7) as the "spatial standard map." It is worth noting that the mapping equations given above are area-preserving.

OVERLAP CRITERION AND STABILITY ANALYSIS

Equation (3) can be rewritten as:

$$\frac{du}{dz} = 2\epsilon \sum_{n=-\infty}^{\infty} cos2\pi(nz - t) \tag{8}$$

For small ϵ ($\epsilon \ll 1$), particles interact with each plane wave, i.e. with each Fourier component of (8), in an essentially independent way. The Hamiltonian for a particle interacting with the n-th wave is:

$$H_n(u, t; z) \ = \ 2\pi n(\sqrt{u} - \frac{1}{n})^2 - 2\epsilon\ sin\zeta \tag{9}$$

where $\zeta = 2\pi(nz - t)$. Clearly, the condition for a particle to interact resonantly with the n-th wave is: $u_n = 1/n^2$. The range of energies over which a particle will be trapped in the n-th wave is given by the trapping width:

$$(\Delta u_{tr})_n \approx \frac{2}{|n|}\sqrt{\frac{2\epsilon}{|n|\pi}} \tag{10}$$

As ϵ is increased the effect of the neighboring waves comes into play as their trapping widths begin to overlap and the above approximations start to break down. The conditions for this to occur is the Chirikov resonance overlap criterion [4] and is given by:

$$(\Delta u_{tr})_n + (\Delta u_{tr})_{n+1} \gtrsim |u_n - u_{n+1}| \tag{11}$$

Using equation (10), this gives the approximate threshold condition for ϵ such that an independent interaction of a particle with a given wave is no longer valid.

$$(\epsilon_{TH})_n \gtrsim \frac{\pi}{8} \frac{(2|n|+1)^2}{|n|(|n|+1)} \frac{1}{[(|n|+1)^{3/2} + |n|^{3/2}]^2} \tag{12}$$

For amplitudes around $(\epsilon_{TH})_n$ stochastic motion will encompass the n-th resonance. For $|n| \gg 1$, the above condition reduces to: $\epsilon_{TH} \gtrsim \pi/(8|n|^3)$. Thus, for any arbitrary small, nonzero, amplitude there will always be a region in energy that is stochastic. However, for any finite amplitude, there will always be a region in energy that does not become stochastic as it would require an infinitely large amplitude to get the $n = 0$ and the $n = 1$ resonances to overlap. A phase-space plot for the spatial standard map is shown in Figure 1 for $\epsilon = 10^{-3}$ and a number of initial conditions distributed in u and t. For this amplitude, the overlap criterion (12) shows that stochasticity exists for $u \lesssim 0.02$. This is approximately the value observed in the graph. The first-order islands corresponding to $n = 2, 3, 4, 5$ and 6 are clearly discernable.

In trying to determine the fixed points of the mapping, T, defined by equations (6, 7) we can, without any loss of generality, choose $\sigma = 1$. Then the fixed points of T are given by

$$u_\ell^* = \frac{1}{\ell^2} \quad \text{and} \quad t_m^* = \frac{(2m+1)}{4} \tag{13}$$

where $\ell = 0, \pm 1, \pm 2, ...$ and $m = 0$ or 1. u_ℓ^* is the same as the wave-particle resonance condition discussed earlier. The stability of these fixed points is determined by the usual methods [3]. Defining:

$$M(u_n, t_n) = \begin{pmatrix} \partial u_{n+1}/\partial u_n & \partial u_{n+1}/\partial t_n \\ \partial t_{n+1}/\partial u_n & \partial t_{n+1}/\partial t_n \end{pmatrix} \tag{14}$$

the stability of u_ℓ^* and t_m^* is given by the criterion:

$$|TrM(u_\ell^*, t_m^*)| \begin{cases} < 2 & \rightarrow \text{stable} \\ > 2 & \rightarrow \text{unstable} \end{cases} \tag{15}$$

where Tr is the trace of the matrix M. All $m = 0$ fixed points are unstable and correspond to hyperbolic points. For $m = 1$, the fixed points are stable (i.e. they are elliptic points) if:

$$\epsilon < \frac{2}{\pi|\ell|^3} \equiv \epsilon_\ell \tag{16}$$

Otherwise, they are unstable. Comparing this with the Chirikov overlap criterion for large ℓ, we find that an elliptic point becomes hyperbolic for an amplitude that is four times larger than is required for the overlap of the island corresponding to that elliptic point with the island of the neighboring elliptic point.

For ϵ slightly greater than ϵ_ℓ, there appear two elliptic points in the phase-space neighborhood of the elliptic point which existed for $\epsilon < \epsilon_\ell$. These are fixed points of T^2 (besides many other fixed points of T^2) which come into existence only after the fixed points of T have become unstable. This illustrates the period doubling sequence of the mapping equations. In Figure 2a we show the surface-of-section plot near the $\ell = 1$ fixed point ($u_1^* = 1, t_1^* = 0.75$) for $\epsilon = 0.63 < \epsilon_1 = 2/\pi$. In Figure 2b $\epsilon = 0.64 > \epsilon_1$, and the period doubling bifurcation has clearly taken place. An analytical determination of the fixed points of T^2 is difficult to carry out as the equations describing the fixed points are transcendental.

DIFFUSION IN ENERGY OF PARTICLE DISTRIBUTIONS

For amplitudes larger than those required for the onset of stochastic motion, it is not possible to give a detailed analytical description of the chaotic particle orbits. However, for practical purposes, this is not necessary. Rather, it is important to have a statistical or a "global" description for the macroscopic evolution of a distribution of particles after a number of interactions with the imposed fields. (For instance, in the case of rf waves interacting with a plasma, one is more concerned with the heating of the plasma, which is a macrosopic effect, than with the intricate microscopic details of the orbits of the particles.) In this section we will describe the statistical properties of the spatial standard map. We will assume that in the stochastic region of phase-space, the wave-phase (t) is randomized much faster than the energy. By averaging over this fast time scale we will be studying the evolution in energy of a distribution of particles after multiple interactions with the external force. In the Fokker-Planck description of the evolution of the distribution function of energy for the Hamiltonian system under consideration, we need to know the diffusion coefficient [3].

We define

$$D_n = \frac{1}{2n}\langle (u_n - u_0)^2 \rangle \tag{17}$$

which is related to the diffusion coefficient, and study its behavior. Here u_n is the energy of a particle after n interactions whose initial energy, u_0, is in the stochastic phase-space. The $\langle \ldots \rangle$ denotes an ensemble average over the wave-phase for a set of particles started at the same energy u_0, but distributed randomly in t. Since the width of the stochastic layer is always finite, u_n is bounded. Thus, in the limit $n \to \infty$, $D_n \to 0$. (In an unbounded, or periodic, phase space which is stochastic, e.g. in the Chirikov-Taylor map, the limit of (17) for $n \to \infty$ would give the conventional diffusion coefficient [5].) The quasilinear diffusion coefficient, which corresponds to $n = 1$, is given by:

$$D_{QL} = \epsilon^2 \qquad \text{for} \ \ u_0 \geq 2\epsilon \tag{18a}$$

and

$$D_{QL} = \epsilon^2 \left[1 - \frac{1}{\pi}\cos^{-1}\left(\frac{u_0}{2\epsilon}\right) - \frac{u_0}{4\pi\epsilon}\sqrt{1 - \left(\frac{u_0}{2\epsilon}\right)^2} \right] \qquad \text{for} \quad u_0 < 2\epsilon \tag{18b}$$

where the expression in (18b) takes into account the reflection of some of the particles as was discussed earlier. This definition of the quasilinear diffusion coefficient assumes that the wave-phase just before the particles interact with the force for the second time is completely uncorrelated with the wave-phase prior to the first interaction i.e. complete phase randomization on each mapping iteration. If this were indeed the case then D_{QL} could be used in the Fokker-Planck equation for the evolution of the distribution function.

In order to decide whether there is phase randomization in one iteration or not, we need to consider the wave-phase correlation function:

$$C_n = \langle (u_n^p - u_{n-1}^p)(u_1^p - u_0^p) \rangle_p \tag{19}$$

where $\langle \ldots \rangle_p$ is an ensemble average over the wave-phase for a set of particles randomly distributed in the stochastic phase-space with u_0^p being the initial energy of the p-th particle. A numerical analysis of C_n shows that there exists an n_c such that for $n > n_c$, C_n is essentially zero for all $\epsilon > 0$. This n_c gives a measure of the number of interactions required with the impulsive force before particles lose memory of their initial conditions. Numerical evaluations of C_n show that $n_c \gg 1$ for all $\epsilon > 0$ so that the basic requirement for the validity of quasilinear theory, namely that $n_c = 1$, is not borne out for the spatial standard map. In fact, for $0 < \epsilon \lesssim 0.1$, $10 \lesssim n_c \lesssim 40$ and for $\epsilon \gtrsim 1.0$ we find that $n_c \gtrsim 70$.

A detailed numerical analysis of D_n as a function of n yields two regimes in amplitude where the behavior of D_n is distinctly different. The two regimes are separated by a critical amplitude, ϵ_c, that is determined to be $\epsilon_c \approx 10^{-3}$. In the first regime, corresponding to $\epsilon < \epsilon_c$, there exists a range of n over which D_n remains essentially independent of n. A typical plot from this regime is shown in Figure 3a where, for $\epsilon = 10^{-5}$, we follow the evolution of a beam of 10^6 particles with $u_0 = 2.56 \times 10^{-6}$. For these parameters $n_c \approx 30$. The approach to this regime of flatness can be either from below (as shown in Figure 3a) or from above depending on the value chosen for u_0 in the stochastic region. In the second regime, where $\epsilon \gtrsim \epsilon_c$, D_n decreases monotonically with increasing n for $n > n_c$. This is shown in Figure 3b where, for $\epsilon = 10^{-2}$, we followed the evolution of 10^6 particles with $u_0 = 10^{-6}$. For this case $n_c \approx 30$.

An explanation of the behavior of D_n in these two regimes and the value of ϵ_c that separates these regimes is best obtained by comparing the spread in energy of an initial beam of particles with the width of the stochastic region. From the resonance overlap criterion (12), we can estimate that for a fixed ϵ, the stochastic region is given by:

$$0 \leq u \lesssim u_b \approx \left(\frac{8}{\pi}\epsilon\right)^{2/3} \tag{20}$$

(This assumes that $|n| \gg 1$ in (12) which is a reasonable approximation for the range of ϵ's we will be discussing in this section.) Furthermore, from (6) the magnitude of the change in energy per interaction with the force is of order ϵ. The average spread in energy of the initial beam during one correlation "time" (i.e. after n_c number of interactions) is $n_c\epsilon$; the width in energy of the stochastic region of phase-space is u_b.

In the case where $n_c\epsilon < u_b$ the beam particles with low initial energies will take, on the average, more than n_c interactions to reach the upper energy boundary of the stochastic region. Here the initial delta-function distribution, $\delta(u-u_0)$, with $u_0 \ll u_b$, first evolves as if the stochastic region were infinite. For $n > n_c$ particles sample different local diffusivities in phase-space (introduced by the non-uniformity in the distribution of phase-space islands discussed earlier), and D_n changes with n. If we define $D_c(u_0)$ as the value of D_n at $n = n_c$ for a fixed u_0, we find that D_c oscillates about D_{QL} as a function of u_0 in the stochastic region. Such a behavior of D_c has been observed before for the Fermi map [6, 7]. We shall not go into further details about $D_c(u_0)$ since the basic ideas explaining its behavior, as discussed in [6, 7], essentially apply to the spatial standard map. As n is increased further, the particle distribution smoothes over these oscillations in $D_c(u_0)$ and D_n remains almost constant as a function of n. The value attained by D_n in this regime is what we shall term as the "global diffusion coefficient." The approach to this global diffusion coefficient with increasing n is from above if the u_0 of the beam is such that $D_c(u_0) > D_{QL}$ and from below for u_0's such that $D_c(u_0) < D_{QL}$. For further increases in n, beyond this region where D_n is flat, D_n decreases monotonically with increasing n (see Figure 3a). This signifies that a majority of the particles have reached the boundaries of the stochastic region and their average energy, and energy spread are no longer increasing. The monotonic decrease of D_n is not proportional to $1/n$ as one would expect if $\langle (u_n - u_0)^2 \rangle$ were not increasing at all. The observed slower rate of decrease of D_n is due to the fact that there are still a lot of particles in the beam that have not reached the higher energy boundary of the stochastic region. The amplitude where $n_c\epsilon \approx u_b$ with $n_c \approx 30$, is approximately $\epsilon \approx 10^{-3} \equiv \epsilon_c$. Thus, this explains the behavior of D_n versus n in Figure 3a. The global diffusion coefficient can be easily read off from the graph to be $D_G \approx 0.95 \times 10^{-10} = 0.95\epsilon^2$. The reason that this value is slightly less than the quasilinear value from (18a) is that, at any interaction with the external force, there are always some particles that are getting reflected. From our numerical computations we find that $D_G \approx 0.95\epsilon^2$ for $\epsilon < \epsilon_c$ provided $u_0 + n_c\epsilon < u_b$ i.e. the initial beam energies are such that in one correlation time the particles in the beam have not reached the upper boundary in energy. For u_0 such that $u_0 + n_c\epsilon \gtrsim u_b$ (and $u_0 < u_b$), D_G is still proportional to ϵ^2 but the constant of proportionality is less than 0.95. In this case many particles in the beam reach the upper energy boundary within one correlation time and cannot gain any further energy due to their stochastic motion. As ϵ approaches ϵ_c from below, there is a decrease in the number of interactions over which D_n remains a constant and D_G becomes less than $0.95\epsilon^2$ independent of $u_0 < u_b$. This is not surprising since as ϵ is increased it takes fewer number of mapping iterations beyond n_c before most of the beam particles have reached their maximum energies.

In the opposite limit of large amplitudes where, $n_c\epsilon \gtrsim u_b$, i.e. $\epsilon \gtrsim \epsilon_c$, the boundary of the stochastic region plays an important role in the determination of the behavior of D_n. Here, within a correlation time, a majority of the particles will have reached the boundaries. Consequently, as argued above, a significant population of the distribution of particles will not be gaining energy or spreading in energy after the first n_c interactions. Indeed, this shows up dramatically in the numerical behavior of D_n as shown in Figure 3b. For $n > n_c$, there is no longer a range of n's over which D_n either increases or remains a constant. In fact, D_n decreases monotonically with n (but slower than $1/n$ for the same reasons discussed above). Furthermore, the increase in n_c for $\epsilon > 0.1$, as mentioned earlier, is due to the boundaries of the stochastic layer. These boundaries reduce the "degrees of freedom" for the particles. For instance, particles at u_b can either remain at u_b or lose energy while those at any other energy in the stochastic layer can either gain or lose energy or remain at the same energy. Since, as ϵ is increased, it takes a fewer number of interactions with the impulsive force to reach energies near u_b the boundary effects begin to dominate and introduce correlations that persist for large values of n.

From this analysis of D_n it is clear that for $\epsilon < \epsilon_c$ the concept of diffusion can be used to describe the dynamics in the stochastic region. For $n > n_c$, D_n changes with n as the diffusion coefficent is a function of the local energies over which the initial beam distribution function is diffusing [6, 7]. For larger values of n, D_n flattens out and remains a constant for a range of n's leading to a global diffusion coefficient which is essentially that given by the quasilinear value (18a).

For amplitudes $\epsilon \gtrsim \epsilon_c$ the dynamics do not seem to be described by the usual concept of diffusion. In this case, as in the previous case, $\langle u_n^2 \rangle$ and $\langle u_n \rangle$ eventually do not change as a function of n indicating that the distribution function of the particles may have evolved to a steady-state where it is no longer changing, on the average, due to further interactions with the impulsive force. However, here the evolution to the steady-state may not be described by the Fokker-Planck equation.

The conclusions arrived at by this model should be valid even when the wavepacket has some finite spatial extent provided it is still small compared to the periodicity length. The effect of finite sized wavepackets remains a subject for future study.

This work was supported in part by the National Science Foundation Grant ECS-8515032 and in part by the Department of Energy Contract No. DE-AC02-78ET-51013.

REFERENCES

1. V. Fuchs, V. Krapchev, A. Ram, and A. Bers, Physica D 14D (1985) 141
2. S. J. Tanaka, Plasma Phys. Contr. Fusion 29 (1987) 1067
3. A. J. Lichtenberg and M. A. Lieberman, *Regular and Stochastic Motion* (Springer-Verlag: New York, Heidelberg and Berlin, 1982)
4. B. V. Chirikov, Phys. Reports 52 (1979) 265
5. A. B. Rechester and R. B. White, Phys. Rev. Lett. 44 (1980) 1586
6. N. W. Murray, M. A. Lieberman, and A. J. Lichtenberg, Phys. Rev. A 32 (1985) 2413
7. A. J. Lichtenberg and M. A. Leiberman, *Diffusion in Two Dimensional Mappings*, Electronics Research Laboratory Memorandum No. UCB/ERL M88/5, University of California, Berkeley, U.S.A. (1988)

Figure Captions

Figure 1. Surface of section plot for the spatial standard map with $\epsilon = 10^{-3}$.

Figure 2. Surface of section plots near the $\ell = 1$ fixed point.

(a) $\epsilon = 0.63$.

(b) $\epsilon = 0.64$ showing the period doubling bifurcation.

Figure 3. D_n versus n for 10^6 particles that are initially distributed uniformly in t. n_c indicates the value of n beyond which the correlation function, C_n, has decayed to zero.

(a) $\epsilon = 10^{-5}$ with the initial energy of the particles in the beam $u_0 = 2.56 \times 10^{-6}$.

(b) $\epsilon = 10^{-2}$, $u_0 = 10^{-6}$.

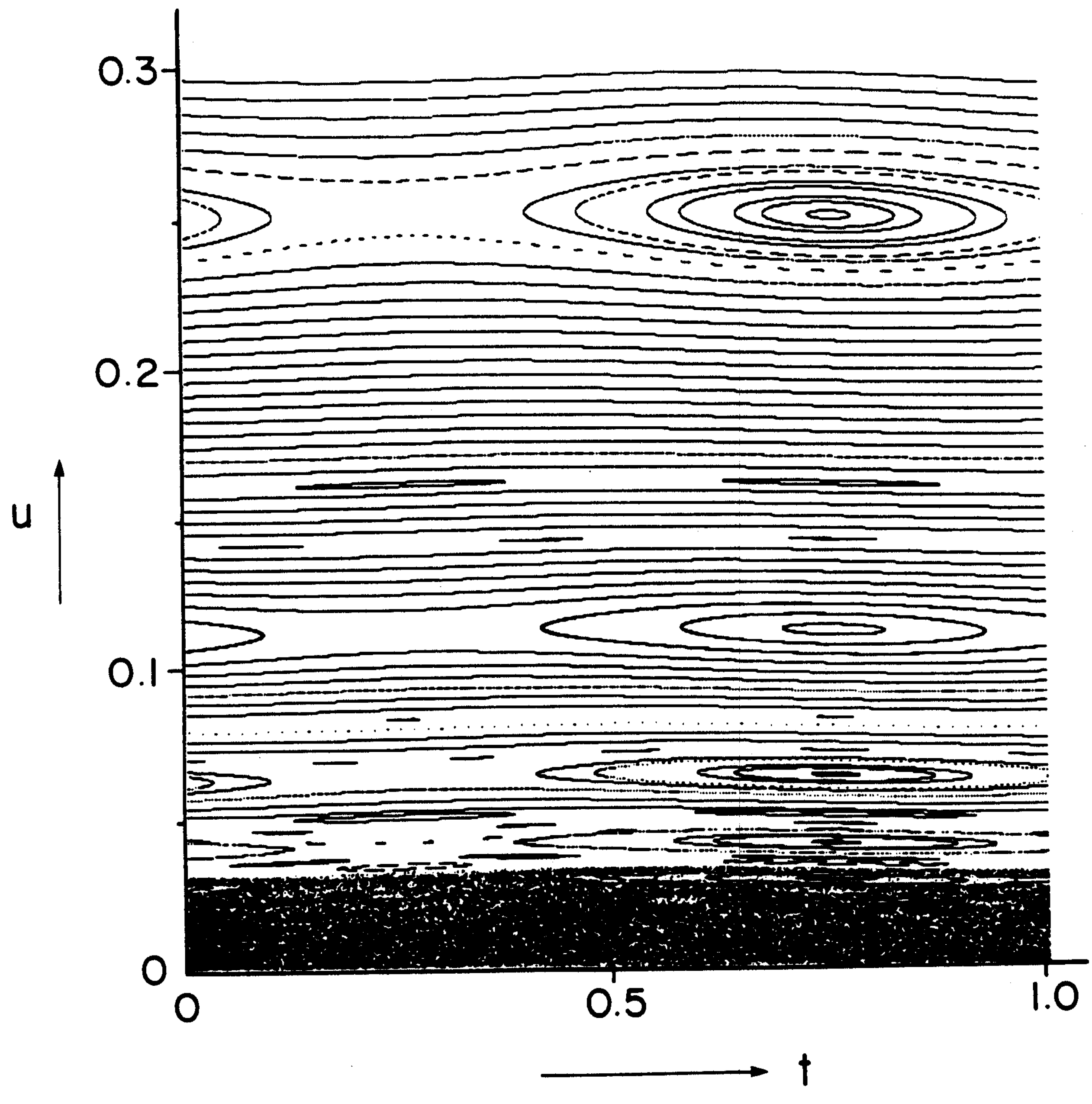

Figure 1

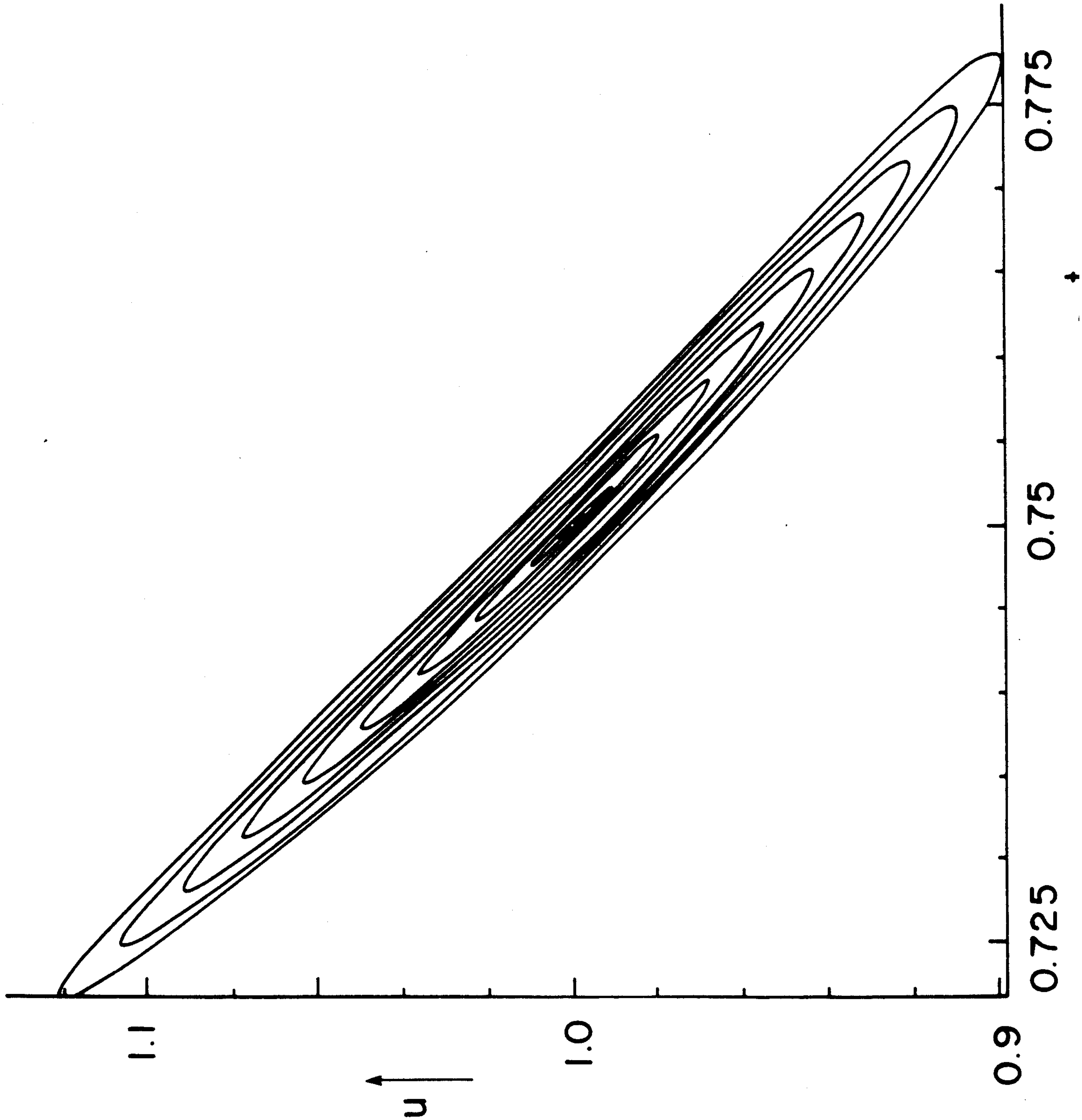

Figure 2a

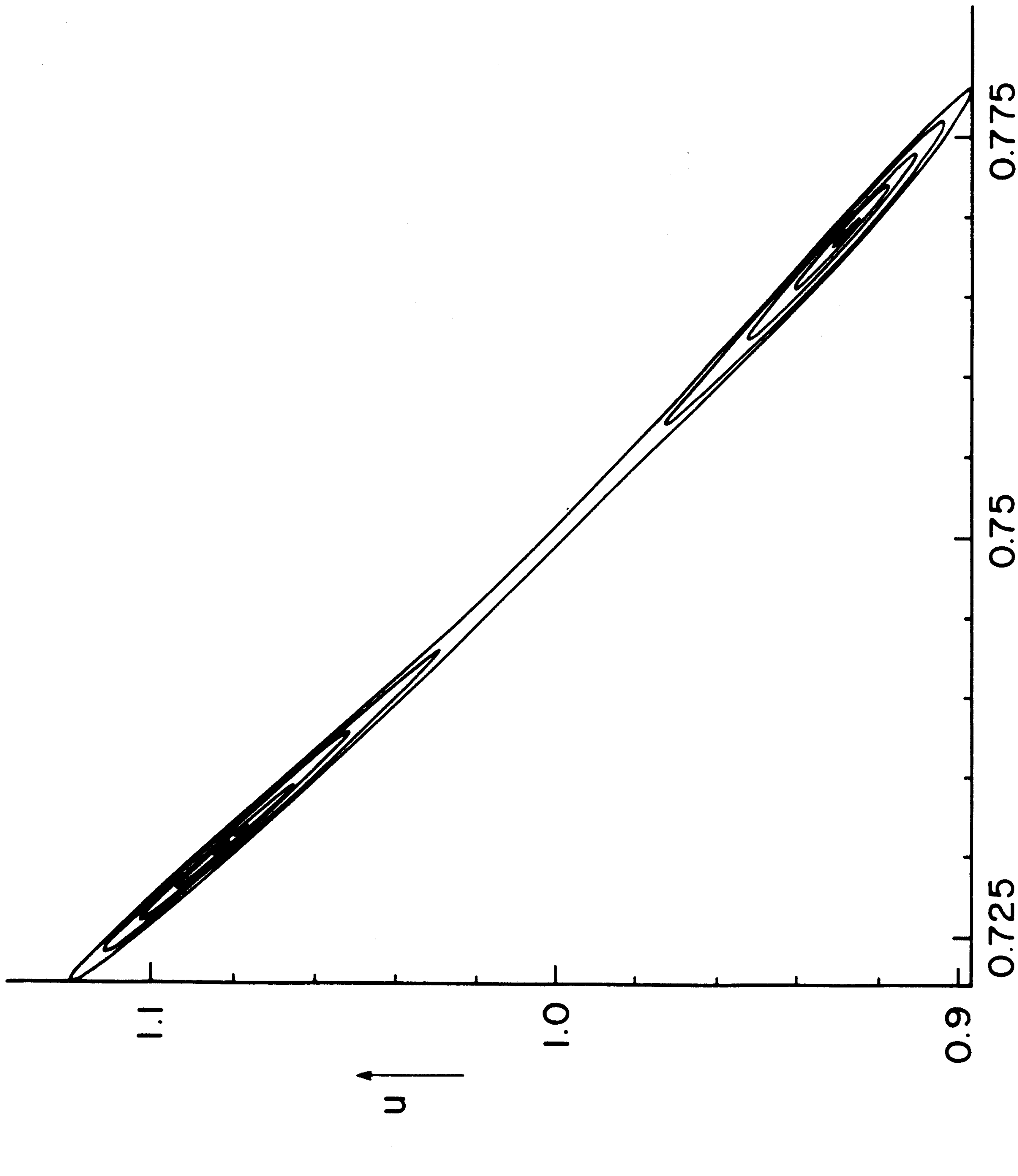

Figure 2b

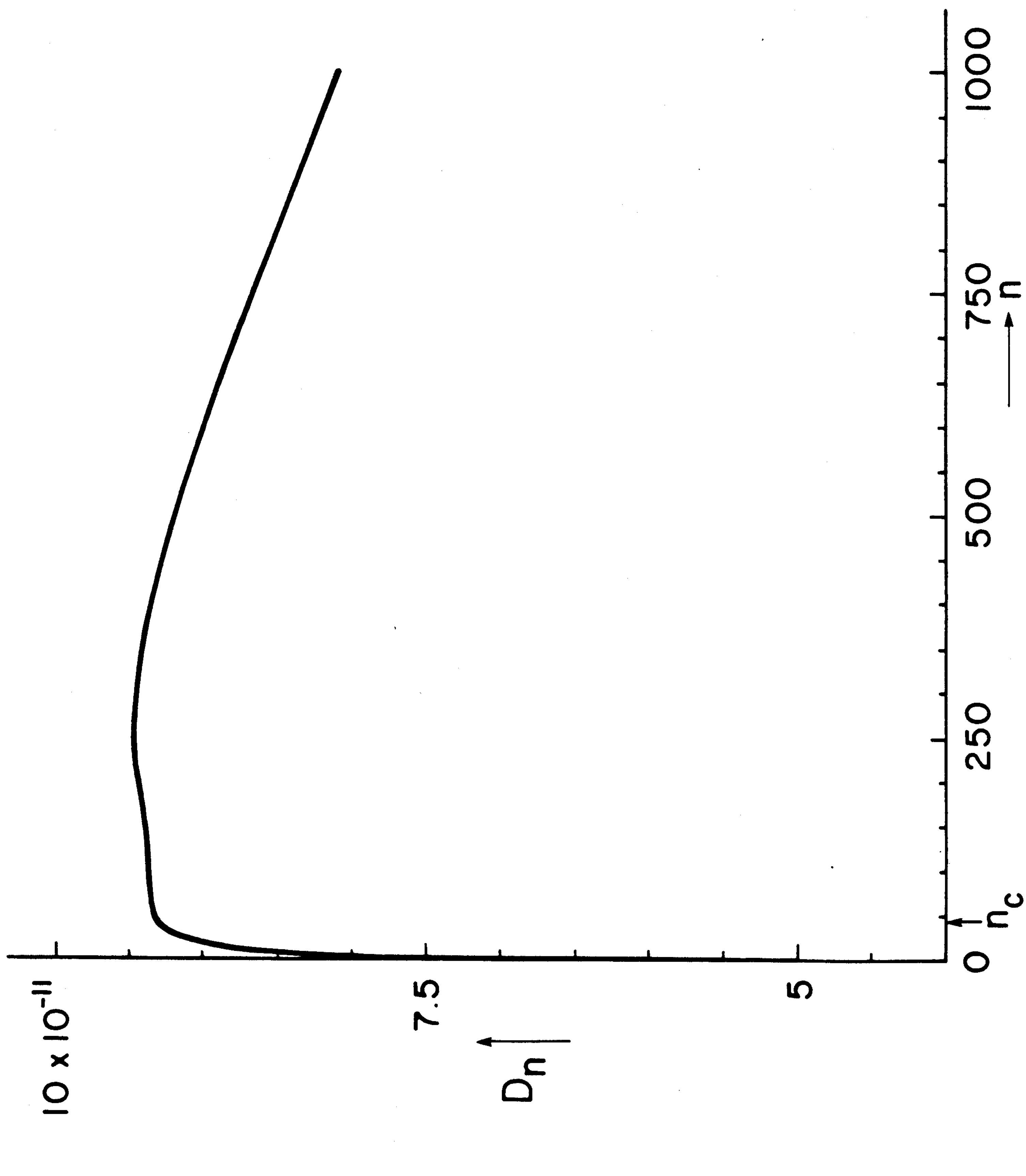

Figure 3a

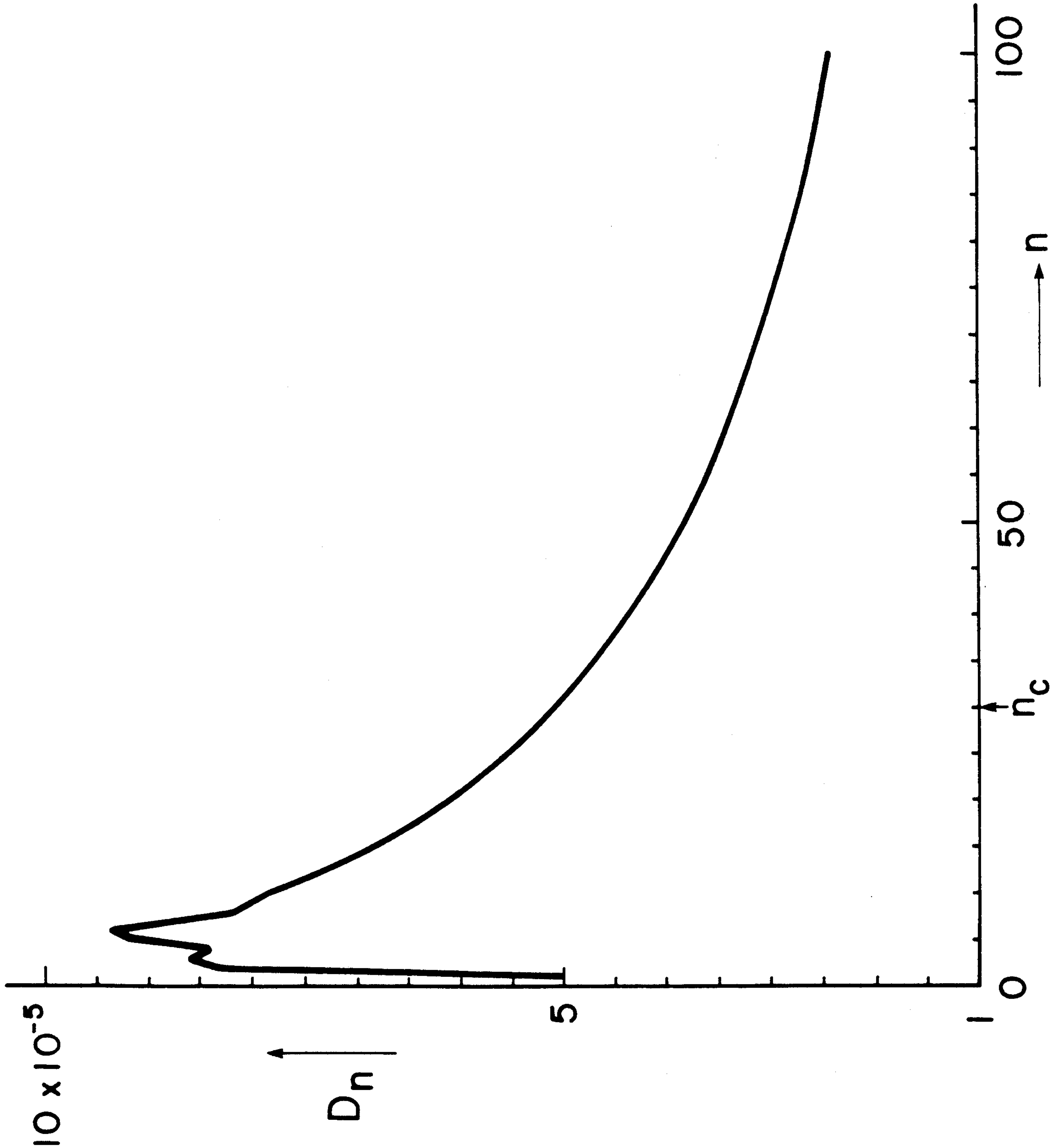

Figure 3b